

Palaeomagnetism of the Late Devonian–Early Carboniferous Achala Batholith, Córdoba, central Argentina: Implications for the apparent polar wander path of Gondwana

Silvana E. Geuna^{a,*}, Leonardo D. Escosteguy^b, Roberto Miró^b

^a CONICET-INGEODAV, Depto. Cs. Geológicas, Facultad de Ciencias Exactas y Naturales, Universidad de Buenos Aires, Pabellón 2, Ciudad Universitaria, C1428EHA Buenos Aires, Argentina

^b Servicio Geológico Minero Argentino (SEGEMAR), Av. Roca 651 Piso 10, C1067ABB Buenos Aires, Argentina

Received 9 May 2006; accepted 7 May 2007

Available online 23 May 2007

Abstract

The Achala Batholith (31°30'S, 64°45'W, Córdoba, Argentina) is a major magmatic complex of the Sierras Pampeanas, emplaced as a post-orogenic pluton in a metamorphic–plutonic basement. It is mainly a porphyritic to coarse-grained equigranular monzogranite, with crystallization age of ~370 and cooling age of ~340 Ma, presently exposed as asymmetric, eastward-tilted blocks. Forty-three sites were sampled in the Achala monzogranite. Overall, it is weakly magnetic, with a mean magnetic susceptibility of 15×10^{-5} (SI). Twenty-two sites showed unstable magnetic behaviour. The remaining 21 sites have haematite as magnetic carrier of a stable remanence. The ilmeno-haematite appears as an accessory mineral, with exsolved intergrowths of (haemo)ilmenite. Thermal demagnetisation up to 620–640 °C isolated steeply-dipping, dual-polarity remanence directions. The palaeomagnetic pole is located at 56°S, 307°E ($N=18$, $A95$ 10.7, K 11). The remanence was locked on cooling, over a range of temperatures from magnetic ordering to exsolution of ilmenite–haematite (~600 to 390 °C). The pole better coincides with the 370–360 Ma segment of the Gondwana apparent polar wander path, suggesting that remanence was acquired quickly. The Achala pole matches a complex mid-Palaeozoic apparent polar wander path (“Y-type”) for Gondwana, which may involve rapid movement, true polar wander episodes and/or continental collisions before the final amalgamation of Pangea.

© 2007 International Association for Gondwana Research. Published by Elsevier B.V. All rights reserved.

Keywords: Palaeomagnetism; South America; Granite; Late Devonian–Early Carboniferous; APWP

1. Introduction

From its assemblage at around 550 Ma to its amalgamation with Laurussia to form Pangea in the latest Palaeozoic, the Gondwana supercontinent seems to have wandered over the South Pole following a complex path, as suggested by the palaeomagnetic poles determined from its main constituent plates, especially Australia, Africa and South America. Many versions of the apparent polar wander path (APWP) proposed for Gondwana (e.g. Morel and Irving, 1978; Kent and Van der Voo, 1990; Chen et al., 1993; McElhinny et al., 2003) share in common the fact of being constituted by several long segments separated by sharp hairpins. Plate reorganization events, true

polar wander episodes, and high plate velocities, have been interpreted on the basis of the length of the APWP segments and the timing of the hairpins (e.g. Meert et al., 1993; Van der Voo, 1993; McElhinny et al., 2003; Evans, 2003; Piper, 2007).

The complexities of the Palaeozoic APWP include a Silurian–Devonian segment defining a loop passing by southern South America. This loop, mainly based on palaeomagnetic poles from eastern Australia, has been questioned by some authors, as it implies a very high drift rate for Gondwana. They proposed, instead, to ignore the Australian poles to generate an APWP passing more or less directly through Africa from the Ordovician to the Carboniferous (e.g. Morel and Irving, 1978; Vêrard et al., 2005).

Palaeomagnetic and rock magnetic studies are presented here on the Achala Batholith, a post-kinematic Late Devonian–Early Carboniferous granitic complex intruded into Late Proterozoic–

* Corresponding author. Tel.: +54 11 45763300x292; fax: +54 11 47883439.

E-mail address: geuna@gl.fcen.uba.ar (S.E. Geuna).

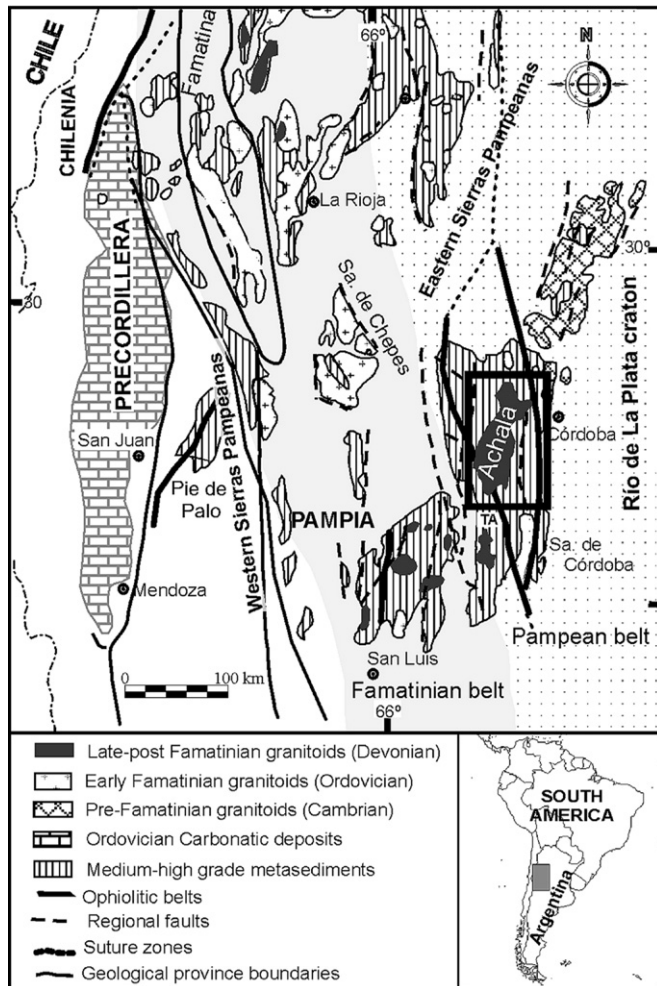


Fig. 1. Generalized map of central Argentina, showing the main areas of Lower Palaeozoic outcrop and terrane boundaries. All of the terranes were accreted to Gondwana prior to the intrusion of the LPO Achala Batholith. TA: Tres Árboles/Guacha Corral shear zone. The inset depicts the location of Fig. 2. Modified from Mutti et al. (2007).

Early Palaeozoic basement forming the Eastern Sierras Pampeanas of Argentina (Fig. 1). Analysis of the magnetic remanence shows that haematite carries a dual-polarity, steep characteristic magnetisation, acquired probably early on cooling of the batholith. The palaeomagnetic pole calculated from the Achala Batholith lies south of southernmost Africa (in a Gondwana reconstruction), in agreement with other palaeomagnetic poles of similar age obtained from Australia, strongly supporting the postulated Silurian–Devonian loop in the Gondwana APWP.

2. Geological setting

The Eastern Sierras Pampeanas are north-trending, west-verging, fault bounded basement uplifts in Central Argentina, consisting mainly of Proterozoic–Early Palaeozoic amphibolite-to granulite-facies metamorphic and plutonic rocks. The basement rocks have been interpreted as belonging to the Río de la Plata craton, metamorphosed due to the accretion of Pampia craton to the west (Kraemer et al., 1995; see Fig. 1), during the Cambrian (Rapela et al., 1998b).

The basement is intruded by Ordovician igneous rocks exposed mainly along the Famatinian belt (see shaded in Fig. 1), marking the inception of a magmatic arc due to further accretion of Cuyania (Precordillera) Terrane (Rapalini, 2005 and references therein).

The Eastern Sierras Pampeanas granitoids have been classified according to their temporal relationship with the main Famatinian deformation episode, into pre-, syn- and late to post-orogenic (Sato et al., 2003; González et al., 2004). The late to post-orogenic (LPO) magmatism is the most abundant, being represented by many subcircular, discordant, high-K plutons (Fig. 1). Geochemically they plot as collisional or intraplate granites, as they show high LIL and HFS (Y–Nb); they developed at great distance from the subduction margin in the later stage of magmatic arc evolution (Rapela et al., 1990). The intrusion of within-plate granites in the Gondwana foreland has been considered as the latest events of the Famatinian Cycle, due to the accretion of the Precordillera terrane to the Gondwana margin (Rapela et al., 1998a; Otamendi et al., 2004) or as a product of a discrete Devonian compressional event (“Achalian orogeny”) linked to the docking of a new terrane, Chilenia, further to the west (Sims et al., 1998; Ramos, 2004; Steenken et al., 2004).

The LPO granites reach batholithic dimensions, in complexes emplaced and cooled quickly, in high-level crust (depths lower than 7.5 km, de Patiño and Patiño Douce, 1987). Porphyritic facies with microcline megacrysts are dominant. They are circular and locally surrounded by undeformed contact metamorphism aureoles. The circular shape can be better described as a polygonal shape that was generated under the brittle conditions of the host rocks; this shape and the characteristics of the aureoles led Pinotti et al. (2002) to favour lateral stopping and fracture propagation instead of ballooning as the main emplacement mechanism for some LPO granites. Thermal modelling applied by Siegesmund et al. (2003) supports an 8 km-thick laccolith shaped body for other “Achalian” granitic complexes.

Compositionally they include calc-alkaline to alkaline, metaluminous to peraluminous granites. Monzogranites–granites are more abundant, with granodiorites, leucogranites and tonalites subordinate. Mafic enclaves, late aplite–pegmatite and lamprophyre dykes are common. U–Pb crystallization ages range from 393 ± 5 (Stuart-Smith et al., 1999) to 368 ± 2 Ma (Dorais et al., 1997).

The Achala Batholith is one of the largest examples of LPO granites; it has an elliptical shape trending N-NE, with a maximum extension of 100×50 km (Fig. 2). Its contacts are regionally sharp and discordant. A limited vertical extension (about 6 km) was supported by a model based on gravity anomalies along a regional transect (Introcaso et al., 1987).

Demange et al. (1996) distinguished five independent magmatic suites, Achala suite being the most extensive (Fig. 2), and suggested that all five suites are nearly coeval but derived from different parental magmatic sources. As a whole, the batholith is a peraluminous, alkali-calcic granitoid developed at great distance from the subduction margin in the later stage of magmatic arc evolution (Rapela et al., 1990).

The most abundant rock type in the batholith is a high-K, coarse-grained to porphyritic monzogranite, with variable

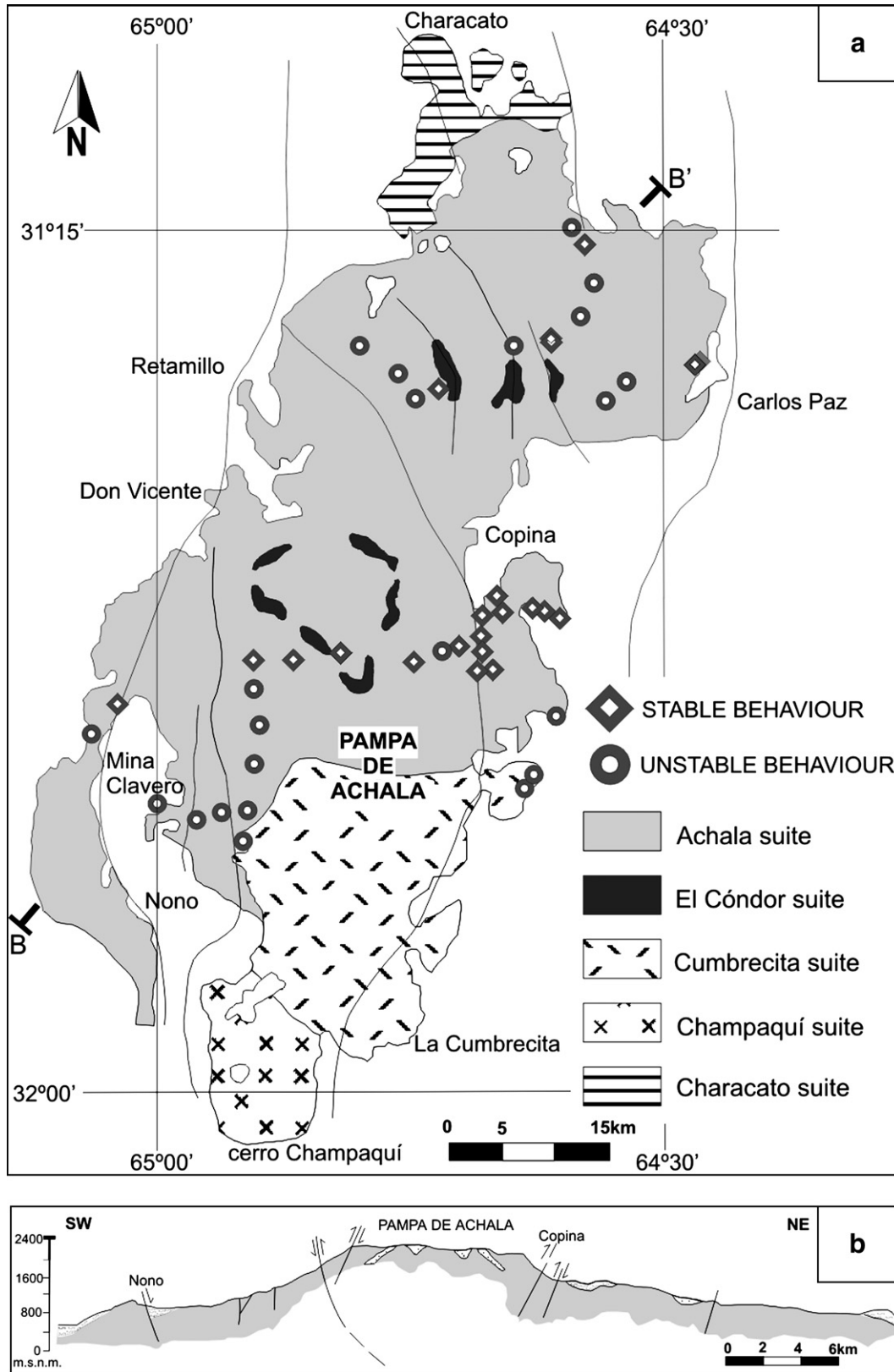


Fig. 2. a) Geological map of Achala Batholith showing the location of the palaeomagnetic sites (modified from Demange et al., 1996). b) Geological section; the top of the granite is a peneplain slightly dipping to the northeast.

amounts of K-spar megacrysts. Plagioclase is often strongly altered to clay minerals and muscovite; magmatic biotite and muscovite are abundant (up to 10 vol.% of the rock). Biotite commonly contains inclusions of apatite, zircon and Fe–Ti oxides, and occasionally may be replaced by late-stage muscovite, haematite, and anatase (Lira et al., 1996).

Microcline megacrysts were formed during the pegmatitic/hydrothermal stage as a result of preferential partitioning of K in a supercritical fluid phase separated from a volatile over-saturated melt (Rapela et al., 1982). Selvage-style greisenization is widespread, developed under temperatures of about 250–350 °C (Lira et al., 1996).

The crystallization age of the main facies was determined by Dorais et al. (1997) in 368 ± 2 Ma, based on analyses of zircons from both the granites and its enclaves. Rb/Sr ages varied from 399 ± 25 Ma (Rapela et al., 1982) to 333 ± 33 Ma (Rapela et al., 1991). The last thermal input in the range 300–400 °C was dated by Jordan et al. (1989) in 336 ± 3 Ma (K–Ar muscovite), implying that the batholith cooled from emplacement temperatures quickly. Rapid cooling, completed in about 30 Ma, was also reported for other LPO granites in the region (Siegesmund et al., 2003).

Subduction-related magmatism had ceased in the central part of Argentina by early Permian time; brittle deformation during regional Carboniferous to Triassic transtensional events initiated major pull-apart basins (Fernandez Seveso and Tankard, 1995). The present structure, where N to NNW oriented uplifted and tilted blocks separate deep sedimentary basins, was formed

by Tertiary to Recent high angle reverse faulting, during the major compressional phase of the Andean Cycle (Jordan and Allmendinger, 1986). The gently-dipping eastern side of the Eastern Sierras Pampeanas blocks has been interpreted as a Gondwanian peneplain (Carignano et al., 1999); Cretaceous–Cainozoic sedimentary rocks covering the basement rocks dip 4 to 12° to the east (Lencinas and Timonieri, 1968).

3. Sampling and laboratory procedures

Palaeomagnetic sampling was performed in the main porphyritic facies of the Achala suite (Fig. 2). Fresh exposures were obtained from road cuts and quarries, as weathering is difficult to avoid everywhere else. One hundred and thirty oriented cylinders (2.5 cm diameter) were collected using a portable, gasoline-powered rock drill at 43 sampling sites, taking 3–4 cores per site. Samples were oriented using both magnetic and sun compasses.

The samples were cut into specimens of 2.2 cm length. Remanent magnetisation was measured using a three-axis 2G DC squid cryogenic magnetometer. Alternating field demagnetisation (AF) was carried out to a maximum of 110 mT (peak) using a static 2G600 demagnetiser attached to the magnetometer. Step-wise thermal demagnetisation up to 680 °C was performed using either a two-chamber ASC or a Schonstedt TSD-1 oven.

At least two specimens from each site were subjected to stepwise demagnetisation, to examine the coercivity and blocking temperature spectra of the natural remanent magnetisation (NRM). As a general procedure, AF demagnetisation was

Table 1
Palaeomagnetic results for Achala Batholith, 31°30'S, 64°45'W, Córdoba, Argentina

Site	N	MS	NRM	Tubl	% 500	P	In situ ChRM				VGP	
							Declination	Inclination	α_{95}	K	Longitude	Latitude
01 ^a	5	8.3	0.6	630/680	100	1.04	330.3	70.7	24.2	10.9	278.6	−0.3
2	5	72.4	19.01	620	95	1.06	40.3	−77.8	3	643.9	92.8	47.6
3	5	20.6	1.74	620	72	1.02	331.6	−81.6	15.3	25.9	126.3	45.6
4	4	19.5	2.29	620/685	100	1.08	297.4	84.3	12.6	54.5	284	−25.9
5	4	8.2	31.41	625	35	1.02	180.9	70.4	14.6	40.4	293.8	−67
15	4	7.8	23.09	640	18	1.03	290.5	−66.6	12.9	51.7	164.7	36.1
20 ^a	3	17.2	7.66	610/650	25	1.04	62.2	66.3	41.6	9.8	331.4	−7.4
21 ^a	3	9.7	1.64	640/680	80	1.06	17.9	−55.9	39.6	10.7	48.1	74.4
22	5	18	4.78	630/675	94	1.1	17.8	−73.6	7	121.9	97.3	59.6
23	4	12.9	2.31	640/680	95	1.06	40	−74.9	12.6	53.9	86.5	50.4
24	3	14.1	6.96	625/680	109	1.04	118.9	−80.2	10.8	131.2	97.3	21.2
26	3	10.3	0.27	635/?	63	1.04	184.2	61.8	15.2	66.8	280.1	−78.1
27	5	17.1	1.34	625/670	90	1.15	133.6	75.1	5.4	201.1	325.5	−47.6
28	4	38.2	45.45	625/675	100	1.08	116.2	67.3	4.9	354.7	343.9	−40
29	4	53.3	5.21	625	27	1.03	192.9	62.2	14.9	39.2	258.2	−74.4
38	5	44.9	21.43	625	120	1.06	129.6	60.1	8.8	77.3	357.3	−48.9
40	5	11.6	1.97	620/680	70	1.03	346.2	−79.2	7.9	94.3	123.2	51.4
42	5	50.6	220.5	615/670	40	1.08	148.7	82.4	5.3	212.1	306	−43.7
46	3	9.9	0.58	615	33	1.04	359.2	−62.9	15.1	67.9	117.9	77
50	4	73.5	31.3	625/670	100	–	157.2	63.3	9.7	89.9	342	−67.9
113	6	7.1	4.58	640	100	–	130.2	74.9	4.5	68.6	326.8	−46.2
Mean	18		Untilted				165	76.2	6.1	32.7	307.1	−56.3
			Tilted to the east								321.9	−54
			Tilted to the north (see text)								305.4	−47.5

N: Number of specimens; MS: Mean magnetic susceptibility $\times 10^{-5}$ (SI); NRM: Intensity of natural remanent magnetisation, mA/m; Tubl: Unblocking temperature as determined from thermal demagnetisation of the NRM; % 500: Fraction of remanence remaining after thermal demagnetisation up to 500 °C; P: anisotropy degree, maximum susceptibility K1/minimum susceptibility K3; ChRM: Characteristic remanent magnetisation; VGP: Virtual geomagnetic pole.

^a Sites excluded for mean direction.

preceded by the application of heating to 150 °C, to eliminate the effects of modern goethite, whereas thermal demagnetisation was preceded by the application of low alternating fields (up to 10–20 mT) to minimize the soft components carried by multidomain magnetite. Bulk magnetic susceptibility was measured after each thermal step in order to monitor possible magnetic mineral changes, by using a MS2W Bartington susceptometer.

Isothermal remanent magnetisation (IRM) up to 4 T was applied to selected samples to identify the minerals carrying the magnetisation. In addition, measurement of low-field thermomagnetic curves was done with a prototype bridge, and anisotropy of magnetic susceptibility (AMS) was measured with a modified Digico susceptometer, at CSIRO facilities in North Ryde (Australia).

Magnetic behaviour of each specimen was analysed by visual inspection of As-Zijderveld plots, stereographic projections and intensity demagnetisation curves. Magnetic components were determined by using principal component analysis (PCA, Kirschvink, 1980), with maximum angular deviation (MAD) values under 15°. Components were determined with at least four consecutive demagnetisation steps.

4. Palaeomagnetic study

Magnetic susceptibility of the Achala main facies is low, ranging from 5 to 150×10^{-5} (SI), what points to magnetite content far below 0.1 vol.%. The NRM is also weak, usually between 0.1 and 5 mA/m, although it can be higher in some sites,

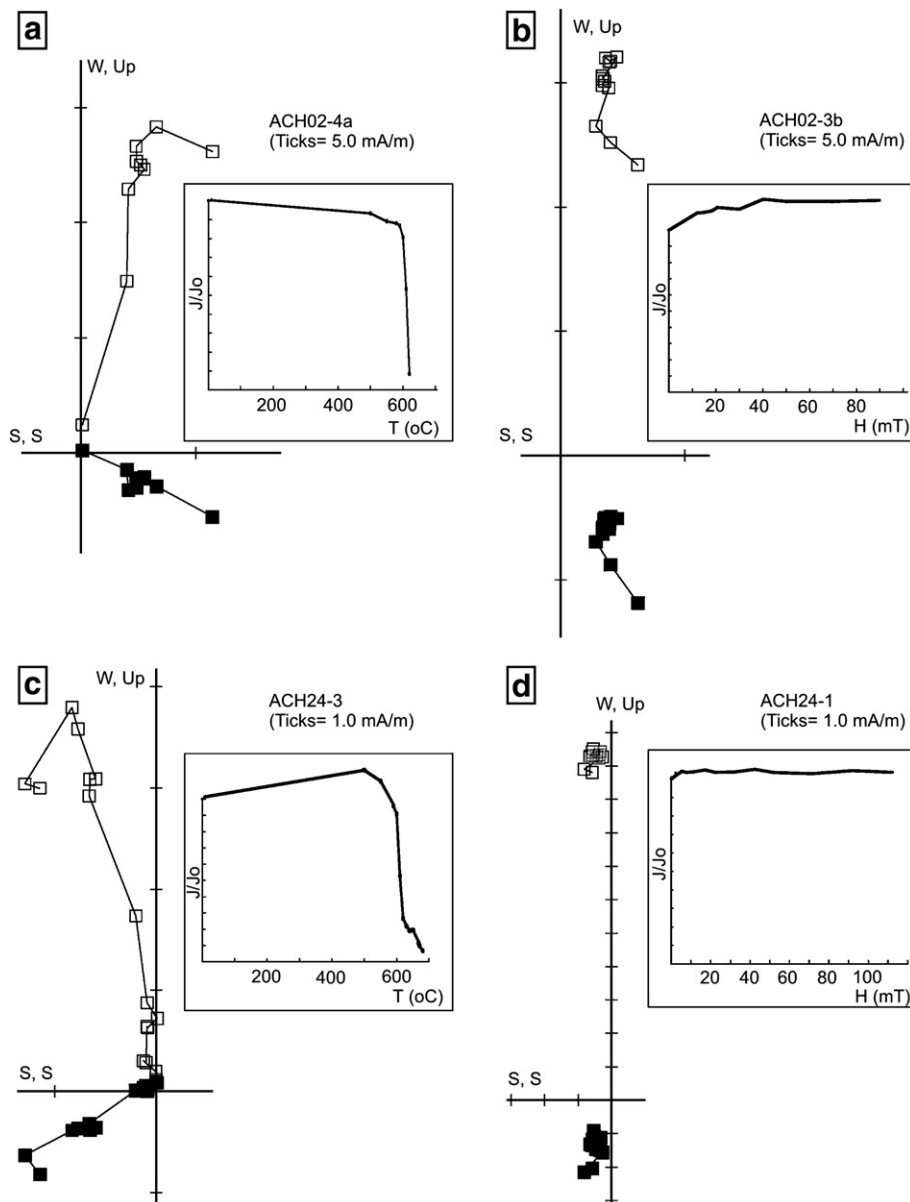


Fig. 3. Examples of typical demagnetisation behaviour in the Achala Batholith, represented by As-Zijderveld orthogonal plots and demagnetisation curves. Open (solid) symbols indicate projection onto the vertical (horizontal) plane. a) Thermal demagnetisation, discrete unblocking temperature; b) and d) AF demagnetisation ineffective; c) thermal demagnetisation, two discrete unblocking temperatures.

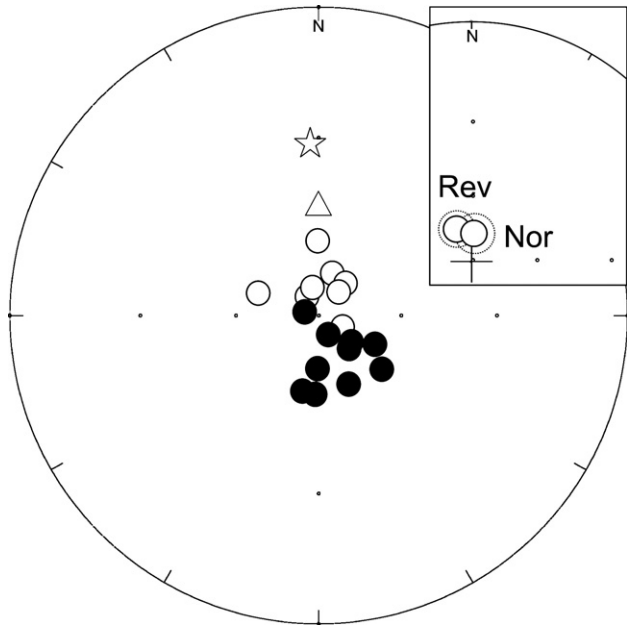


Fig. 4. Palaeomagnetic *in situ* site mean directions in stereographic projection. Open (solid) symbols indicate negative (positive) inclination. Inset depicts a positive (class C) reversal test for these palaeomagnetic data (reversed directions inverted into normal directions, the outer circles represent the 95% confidence cone). The star and the triangle represent the present and dipolar magnetic field in the sampling area, respectively.

reaching up to 200 mA/m. Two kinds of behaviour were observed during demagnetisation, as follows (see locations for sites in Fig. 2):

- Unstable behaviour. It characterizes about half of the sites (22), usually those with lower NRM intensity (0.1 to 2 mA/m). Remanence of these samples became erratic after demagnetisation to 25 mT or 300 °C. Components determined before these steps showed no within-site consistency.
- Stable behaviour. For the remaining 21 sites, AF demagnetisation was effective only to remove a fraction of the remanence carried by a trace amount of magnetite. The fraction removed varied from 0 to 80% (Table 1), but was usually less than 25%. The soft component eliminated this way showed inconsistency within sites.

In stable samples, the NRM remaining after 15 mT was completely unaffected by AF demagnetisation, revealing coercive forces far higher than 100 mT (Fig. 3). On the other side, thermal demagnetisation resulted in blocky curves with discrete unblocking temperatures of 610–640 °C (Fig. 3a), sometimes followed by a second step around 670–680 °C (Fig. 3c). The magnetic components determined by thermal demagnetisation up to these temperatures (“A” components) were fully consistent within sites; only one high temperature component was determined on each

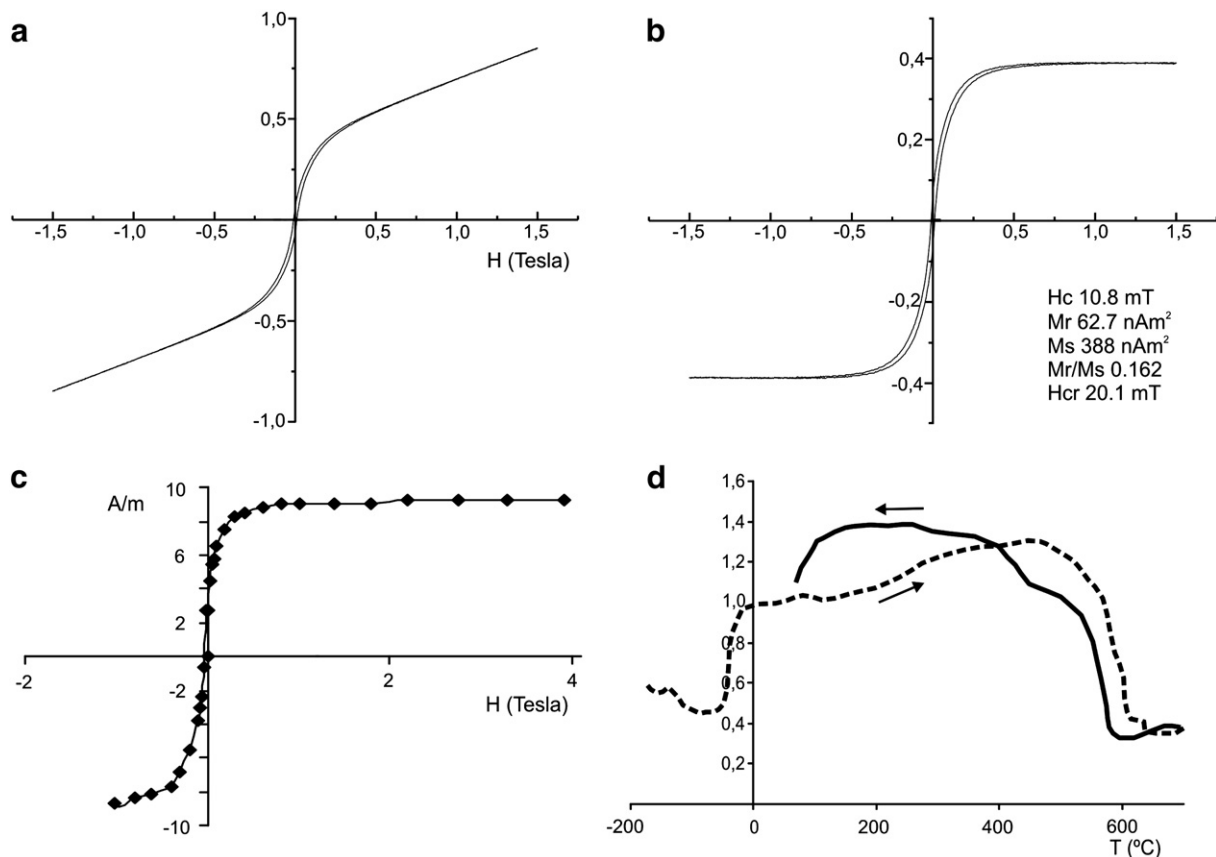


Fig. 5. a) Uncorrected hysteresis curve; b) Hysteresis curve after correction for paramagnetic content; c) Isothermal remanence acquisition curve and backfield; d) Low-field thermomagnetic (magnetic susceptibility k vs. T) curve. Dashed and solid lines represent heating and cooling thermomagnetic curves respectively, after subtraction of paramagnetic susceptibility. All samples from site 2.

sample, even if they showed more than one unblocking temperature (i.e., no directional changes were observed, the whole spectra of unblocking temperatures carry the same component of magnetisation).

Site mean directions were calculated for the A components isolated in the 21 sites showing stable behaviour. Three of these sites show poor grouping of directions (means with low values of the statistical parameter k), and were discarded for subsequent analysis. The remaining 18 sites provided good quality steeply-dipping, dual-polarity remanence directions (Fig. 4, Table 1).

A reversal test applied to 10 down-dipping and 8 up-dipping directions was positive, class “C” (McFadden and McElhinny, 1990). The virtual geomagnetic poles calculated from the 18 sites defined a population with an angular dispersion (S) of 24°. A palaeomagnetic pole was calculated from it, at 56°S, 307°E, A95 10.7, K 11 ($N=18$).

5. Magnetic petrology

IRM acquisition and hysteresis curves of representative samples were dominated by the response of trace amounts of magnetite, as this low-coercive mineral is much more sensitive to high field experiments (Fig. 5a, b, c). However, low-field k - T curves show the presence of a mineral with Curie–Néel temperature of 620 °C, and a decay around –30 °C that can be attributed to the Morin transition of haematite (Fig. 5d).

AMS was measured for all the specimens before the demagnetisation procedures. Anisotropy degree (P) varies between 1.016 and 1.149, most of the sites showing P lower than 1.1. K3 coincides with the pole to magmatic foliation in every case the latter could be observed (Geuna et al., submitted for publication). In all cases, the anisotropy degree is low enough to rule out any distortion of the palaeomagnetic vector.

Low susceptibility values, high coercivity and high unblocking/Curie–Néel temperatures, altogether point to haematite as the mineral carrying the remanent magnetisation of the Achala suite. In pure haematite, the change to the antiferromagnetically ordered structure occurs at a Néel temperature of 680 °C, but this temperature falls rapidly to about 450 °C for a composition of Ilm_{25} . Therefore the Néel or Curie temperature of 610–640 °C as observed, can be interpreted as an indication of the presence of ilmenite (FeTiO_3) in the haematite of the Achala suite, in an amount no higher than 10%. The second unblocking temperature of 670–680 °C observed in some samples indicates the presence of a pure haematite fraction.

Preliminary microscopic observation of polished sections permitted the identification of well developed titanohaematite grains in samples representative of sites carrying the A component. At least two generations of ilmenite exsolution lamellae can be observed optically within them, as fine lamellae parallel to $\{0001\}$. Locally, minor late-stage oxidation at temperatures below 400 °C is evident by the oxidation reaction of ilmenite to haematite+rutile±spinel. No magnetite was observed. On the other side, samples representative of sites with unstable behaviour showed virtual absence of primary opaque oxides and a high degree of meteoric alteration.

6. Discussion

6.1. Remanence acquisition

Half of the sites sampled in the Achala suite’s main facies showed a stable, dual-polarity magnetic remanence carried by haematite with a limited amount of Ti in its structure, as it was interpreted from the analysis of the demagnetisation procedures. Textures observed under optical microscope show that haematite is present in the granite almost exclusively as a product of exsolution from a member of the haematite–ilmenite solid solution ($\text{hem-ilm}_{\text{ss}}$) series. Unblocking temperatures are roughly consistent with a haematite-rich component of the intergrowths.

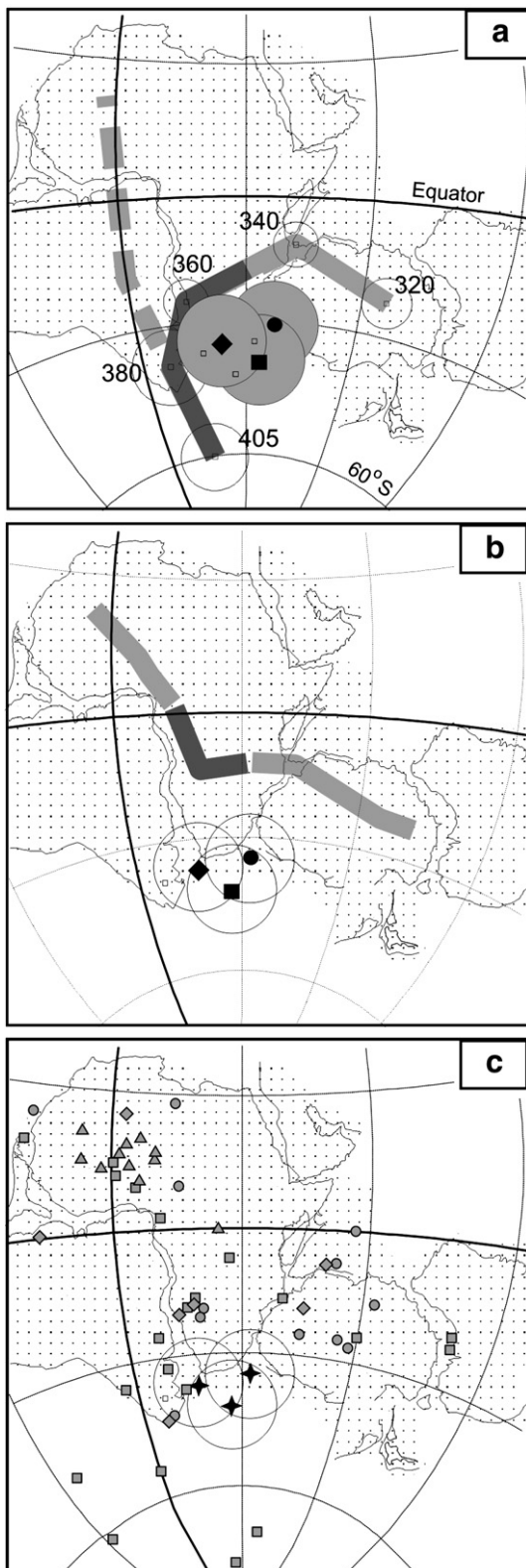
It has been long recognised that haematite and ilmenite form a continuous solid solution series at high temperature (e.g. Robinson et al., 2004 and references therein). On slow-cooling the separation of haematite and ilmenite occurs, and also the antiferromagnetic ordering of the Fe-rich member. The effect of both processes on the magnetic properties depends on the bulk initial composition. In pure haematite, the change to the antiferromagnetically ordered structure occurs at a Néel temperature of 680 °C, but this temperature falls rapidly to about 450 °C for a composition of Ilm_{25} . It means that, while Fe-rich oxides will acquire antiferromagnetic ordering at high temperatures (680 °C for pure haematite), Ti-rich oxides will only acquire magnetic ordering at lower temperatures, and the magnetic phase will be the exsolving haematite, preferentially at the eutectoid temperature of 390 °C (Robinson et al., 2004).

Experimentally determined Néel temperature of about 610–640 °C is related to the present composition of the exsolved end-member haematite, which would contain less than 10% Ti. However, the original Fe–Ti oxide bulk composition is unknown, and so is the temperature at which antiferromagnetic ordering was formerly acquired. We are only certain that the temperature was lower than 610 °C (as the original oxide was Ti-richer than the present end-member haematite) and not much lower than 390 °C (the eutectoid temperature at which most of the exsolution occurs).

It is clear then that Ti-rich oxides would acquire their magnetic remanence at temperatures substantially lower than the Néel temperatures of the end-member components. However, once the magnetic ordering was attained and hence the remanence blocked, this remanence could only be removed by 1) applying temperatures as high as the Curie–Néel point of the end-member, which can reach 680 °C or 2) creating the conditions as to dissolve again the haematite-rich phase (McEnroe et al., 2001).

In summary, the nature of the magnetic minerals indicates that magnetic remanence of the Achala suite would have been acquired on cooling, approximately at the time when the intrusive body cooled from 610° to 390 °C. This would be at any moment between crystallization (368 Ma) and the closure of the K–Ar system in muscovite (336 Ma). Once blocked, magnetic remanence would have been very resistant to low temperature remagnetisation events.

The recording of both polarities confirms that palaeosecular variation was averaged out; this could be attributed either to slow-cooling during a magnetic reversal, or to the sampling of several pulses of magmatic intrusion in the batholith. Low anisotropy degree and magmatic fabric also indicates lack of remanence deformation.



6.2. Palaeohorizontal determination

The post-orogenic Achala Batholith is presently exposed at the top of the range blocks, which are modelled as planated surfaces known as “pampas” (Fig. 2b). According to Carignano et al. (1999), the large and well developed planated surfaces formed originally in response to degradation occurred in the Late Jurassic–Late Cretaceous interval. These surfaces, tilted gently to the east during the Andean Cycle in the Cainozoic, expose cupola structures roughly representing the original intrusion geometry.

The top of the batholith does not seem to differ significantly from the horizontal plane at the moment of the emplacement, judging from the presence of abundant subhorizontal pegmatite and aplite dykes, probably emplaced in relief fractures in the complex, which should have been horizontal at that time. Also roof contacts are exposed in many places, especially in the NE and SW blocks. Given the huge dimensions of the blocks at surface, and considering as valid the gravity-based interpretation of Introcaso et al. (1987) of a limited extension at depth to about 6 km, any departure from the horizontal should cause the exposure of the roots of the batholith. No change in mineralogy and facies has been observed that could be associated to such a variation in depth exposure.

The Achala Batholith was emplaced following the Guacha Corral/Tres Árboles shear zone, interpreted as a major tectonic boundary related to Pampia–Río de la Plata collision (Kraemer et al., 1995). Although controlled by this high strain zone, the batholith is undeformed, clearly postdating the main deformation events.

However, Permian–Cretaceous and Tertiary brittle faults are most likely responsible for later reorientation of the blocks. According to Simpson et al. (2001), block rotation about a horizontal axis is a significant component of the N–S trending Neogene faults, as evidenced by the 1000 m scarp of the western edge of the Achala block (Fig. 2b). The batholith resulting in a final horizontal position is consistent with movement along listric faults, active first in the Cretaceous as normal faults. The reversal of the slip on a single fault trace during successive reactivations resulted in a small net displacement. Another sign of small net displacement due to reactivation is the continuity of metamorphic isograds in basement rocks on both sides of the younger faults (Simpson et al., 2001). Finally, the Mesozoic–Cainozoic sediments overlying the range blocks have a regional dip of 4–12° to the east (Lencinas and Timonieri, 1968).

Fig. 6. Palaeozoic APWP for Gondwana; Devonian segment is shown in darker grey colour. a) Y path, pole selection after McElhinny et al. (2003). Gondwana reconstruction parameters after Lawver and Scotese (1987). Poles combined by using the method of McFadden and McElhinny (1995). Achala pole versions are shown with the 95% confidence circle grey-shaded. Square, diamond and circle represent the results for untilted, 5° tilted to the north and 5° tilted to the east, respectively. b) X path for Gondwana APWP, running more or less directly through Africa during the mid-Palaeozoic. Gondwana position with Africa fixed is shown for reference. c) Palaeomagnetic poles used to construct the APWPs in a) and b), transferred to African coordinates using Lawver and Scotese (1987) reconstruction parameters. Achala poles shown as stars for comparison. Squares: poles from Australia; circles: poles from Africa; triangles: poles from East Antarctica; diamonds: poles from South America.

Achala granite at the present outcropping exposure level has not undergone major significant displacement, neither by post-Devonian orogenic events nor by the most recent compressional Andean faulting cycle. We concluded that the structural uncertainty is clearly below 10° and that it does not affect the main conclusions to be arrived.

As the influence of appreciable later tilting on the remanence can be ruled out, we decided to interpret all mean directions as *in situ*. Alternatively, we could use a conservative approach and consider results including a reasonable amount of tilting around the most probable tilting directions according to the geology, that is 5° of tilting, to the north and to the east (Fig. 6). Although we prefer the *in situ* interpretation, the alternative results put a somewhat speculative but reasonable limit to the uncertainty involved when considering the application of minor tectonic corrections.

6.3. Palaeopole position and geodynamic implications for Gondwana

Although the first arc-continent and continent–continent collisions leading to the agglutination of Gondwana may have started more or less simultaneously to the later episodes of rifting of parts of Rodinia, at about 880–930 Ma, the final stage of the polyphase accretion of Gondwana would not have occurred until 550–530 Ma (Meert, 2001, 2003; Cordani et al., 2003). Since then and during the rest of the Palaeozoic, the Gondwana movement over the South Pole has followed a complex path, as defined from palaeomagnetic poles.

The APWP of Gondwana for the Middle–Late Palaeozoic, when plotted in a Gondwana reconstruction, defines a track from the vicinity of Chile to west-central Africa and then to Antarctica, from Late Silurian to Late Carboniferous (Fig. 6a). The details of the Palaeozoic segment of the APWP of Gondwana should bring information about Palaeozoic plate movements, which in turn involve the demise of oceans such as Iapetus and the late Palaeozoic assembly of Pangea. For example, the large swings described by the APWP have been the focus of attention and controversy, as they imply high plate velocities for Gondwana, very extreme climatic variations, and possible Silurian–Devonian collisions between Gondwana and other continents (Van der Voo, 1993).

Simpler paths have been proposed by ignoring the Silurian to Early Devonian palaeopoles from eastern Australia and the African Air pole (Fig. 6b). This group of APWPs includes the “X path” proposed originally by Morel and Irving (1978), refined by Van der Voo (1993) and recently supported by V  rard et al. (2005). In this option, the first loop in Fig. 6a is omitted, which rules out a mid-Palaeozoic continent–continent collision involving Gondwana, as the pole moves slowly from a location near northwest Africa in the Ordovician to a west-central African location in the Devonian. It means that Gondwana remains separated by a wide ocean from Laurentia and Baltica until after the Devonian (Van der Voo, 1993).

The simple, direct X path contrasts with the complex Y path concept of Morel and Irving (1978), successively supported by Schmidt et al. (1990), Li et al. (1993) and Anderson et al. (2004), among others; one of its latest versions, presented by McElhinny

et al. (2003), is depicted in Fig. 6a. As all loops are considered, the Y path implies velocities for Gondwana displacement with respect to the pole which are faster than continental motions observed today. The rapid continental drift might be true fast motion for Gondwana, driven by thermal buoyancy generated via mantle plumes beneath supercontinents (Meert and Tamrat, 2004). However, at least part of the displacement could be attributed to true polar wander, as it has been proposed by Van der Voo (1994), Evans (2003) and Piper (2007). In any case, the Y path implies that Laurentia and Gondwana might have collided during the Late Silurian to Early Devonian (Acadian orogeny), but this did not result in a lasting supercontinent of a Pangea configuration, as the Devonian palaeopoles near central Africa indicate that Gondwana went back to the south, away from Laurentia. The Devonian ocean between the two continents is thought to have closed during the Carboniferous, resulting in the Hercynian–Alleghenian orogeny and the formation of Pangea (e.g. Van der Voo, 1993).

Due to the paucity of the palaeomagnetic record in the Silurian–Devonian for Gondwana, the distinction between X, Y and other paths is still an open question. As an example, V  rard et al. (2005) have interpreted their Devonian Australian results as better supporting the X (direct) path, although their conclusion is based on a pole clearly not averaging the palaeosecular variation. Among the implications of their result, V  rard et al. (2005) proposed that Y path might be an artifact due to block rotations in the eastern Lachlan Orogen.

When compared to the Gondwana APWP after reconstruction based on the Lawver and Scotese (1987) parameters, all three versions of the Achala pole (untilted, tilted to the north and tilted to the east) better coincide with the segment ~370–365 Ma of the “Y-type” Gondwana APWP (Fig. 6a). In particular, the Achala pole is coincident with a pole calculated from red beds of the Worange Point Formation, Eastern Australia, dated in 365 Ma (Thrupp et al., 1991). On the other side, the Achala pole is not coincident with any segment of the “X-type” APWP (Fig. 6b).

None of the Achala pole versions can be reconciled with the Gondwana reference pole for 340 Ma, the Achala cooling age for muscovite, for any of the paths proposed. The better agreement with older poles would mean that haematite likely acquired its remanence at higher temperatures than the 390 °C eutectoid proposed by Robinson et al. (2004), and therefore at a moment closer to the crystallization age of ~370 Ma.

The “Y-type” paths are strongly based on pre-Carboniferous results from Eastern Australia, which have been questioned by its possible non-cratonic nature (e.g. V  rard et al., 2005). The Achala pole, coming from the Sierras Pampeanas de C  rdoba, a belt attached to cratonic South America since the Cambrian (Rapela et al., 1998b), lends strong support for the “Y-type” path.

7. Conclusions

– Experimental work has led us to the conclusion that haematite is the main magnetic mineral of the Achala Batholith. The ubiquitous presence of ilmenohaematite, and the rare occurrence (absence?) of magnetite, is supported by thermal and

alternating field demagnetisation studies, saturation magnetisation measurements, hysteresis properties, and temperature-hysteresis studies.

- The remanence carried by haematite must have been locked on cooling, in the temperature range 610°–390 °C, the lower being the eutectoid temperature proposed by Robinson et al. (2004). Crystallization age of the batholith is ~370 Ma (Dorais et al., 1997), and cooling age to 300–400 °C is indicated by a K–Ar muscovite age of ~340 Ma (Jordan et al., 1989).
- Remanence deformation can be discarded as magnetic fabric is weakly anisotropic. A positive reversal test indicates that palaeosecular variation was averaged during the construction/cooling history of the batholith. Furthermore, the nature of magnetic mineralogy seems refractory to remagnetisation events, as end-member haematite shows extremely high coercivity once exsolved.
- The batholith postdates the main deformation events in the region; it was emplaced in the Devonian Gondwana foreland as a post-orogenic intrusion. A palaeomagnetic pole was calculated considering that the batholith present position is nearly horizontal; the influence of an eventual tectonic correction was analysed and it was concluded that, though introducing additional uncertainty, the correction does not affect the main conclusions.
- The untilted Achala palaeomagnetic pole is at 56°S, 307°E ($N=18$, $A_{95} 10.7$, $K 11$). It better coincides with the 370–365 Ma segment of the Gondwana APWP. We interpret that remanence blocking in haematite was produced at temperatures higher than 390 °C, and therefore the pole age is closer to the crystallization age (~370 Ma) than to the closure of the K–Ar system in muscovite (~340 Ma).
- The Achala palaeopole favours a complex “Y-type” APWP for Gondwana, instead of a simpler “X-type” as proposed by Vêrad et al. (2005). This lends support for the Devonian–Carboniferous poles from Eastern Australia, as the Y-type paths are strongly based on them. The complexity in the mid-Palaeozoic APWP should be interpreted in terms of continent–continent collisions (Acadian orogeny, e.g. Van der Voo, 1993) and/or of oscillatory, multiple true polar wander (e.g. Evans, 2003).

Acknowledgements

This work was partially supported by grants from: ANPCyT (BID 1201/OC-AR-PICT 07-10602), MECyT (IM40-2000 No. 61) and CONICET (PIP 5783). Argentine Geological Survey (SEGEMAR) provided assistance in the fieldwork. F. Gaido and J.C. Candiani contributed to the selection of the sites. Some experiments were carried out in the CSIRO facilities at North Ryde, as part of a CONICET fellowship to SG. Kind assistance of D. Clark, P. Schmidt and M. Huddleston is acknowledged. We are also grateful to S. McEnroe, D. Mutti, and S. Singer for fruitful discussions about the samples. R. Tomezzoli, A. Rapalini, C. Mpodozis, J. Meert and A. Vaughan are thanked for reviews that helped to improve the manuscript. This paper is a contribution to the IGCP Project 471 “Evolution of Western Gondwana during the Late Paleozoic: tectonosedimentary record, paleoclimates, and biological changes”.

References

- Anderson, K.L., Lackie, M.A., Clark, D.A., 2004. Palaeomagnetic results from the Palaeozoic basement of the southern Drummond Basin, central Queensland, Australia. *Geophysical Journal International* 159, 473–485.
- Carignano, C., Cioccale, M., Rabassa, J., 1999. Landscape antiquity of the Central-Eastern Sierras Pampeanas (Argentina): geomorphological evolution since Gondwanic times. *Zeitschrift für Geomorphologie. NF Supplementbände*, vol. 118, pp. 245–268.
- Chen, Z., Li, Z.X., Powell, C.McA., Balme, B.E., 1993. Palaeomagnetism of the Brewer Conglomerate in central Australia, and fast movement of Gondwanaland during the Late Devonian. *Geophysical Journal International* 115, 564–574.
- Cordani, U.G., Brito-Neves, B.B., D’Agrella-Filho, M.S., 2003. From Rodinia to Gondwana: a review of the available evidence from South America. *Gondwana Research* 6 (2), 275–283.
- Demange, M., Álvarez, J.O., López, L., Zarco, J.J., 1996. The Achala Batholith (Córdoba, Argentina): a composite intrusion made of five independent magmatic suites. Magmatic evolution and deuteritic alteration. *Journal of South American Earth Sciences* 9 (1–2), 11–25.
- de Patiño, M.G., Patiño Douce, A.E., 1987. Petrología y petrogénesis del Batolito de Achala, provincia de Córdoba, a la luz de la evidencia de campo. *Revista de la Asociación Geológica Argentina* 42 (1–2), 201–205.
- Dorais, M.J., Lira, R., Chen, Y., Tingey, D., 1997. Origin of biotite–apatite rich enclaves, Achala batholith, Argentina. *Contributions to Mineralogy and Petrology* 130, 31–46.
- Evans, D.A.D., 2003. True polar wander and supercontinents. *Tectonophysics* 362, 303–320.
- Fernández Seveso, F., Tankard, A.J., 1995. Tectonics and stratigraphy of the Late Paleozoic Paganzo basin of western Argentina and its regional implications. In: Tankard, A.J., Suárez Soruco, R., Welsink, H.J. (Eds.), *Petroleum basins of South America*. American Association of Petroleum Geologists, Memoir, vol. 62, pp. 285–301.
- Geuna, S.E., Escosteguy, L.D., Miró, R., Candiani, J.C., Gaido, M.F., submitted for publication. La susceptibilidad magnética del batolito de Achala (Devónico, Sierra Grande de Córdoba): datos preliminares y comparación con otros granitos “Achalianos”. *Revista de la Asociación Geológica Argentina*.
- González, P.D., Sato, A.M., Llambías, E.J., Basei, M.A.S., Vlach, S.R.F., 2004. Early Paleozoic structural and metamorphic evolution of Western Sierra de San Luis (Argentina), in relation to Cuyania accretion. *Gondwana Research* 7 (4), 1157–1170.
- Introcaso, A., Lion, A., Ramos, V.A., 1987. La estructura profunda de las sierras de Córdoba. *Revista de la Asociación Geológica Argentina* 42 (1–2), 177–187.
- Jordan, T.E., Allmendinger, R.W., 1986. The Sierras Pampeanas of Argentina: a modern analogue of Rocky Mountain foreland deformation. *American Journal of Science* 286, 737–764.
- Jordan, T.E., Zeitler, P., Ramos, V., Gleadow, A.J.W., 1989. Thermochronometric data on the development of the basement peneplain in the Sierras Pampeanas, Argentina. *Journal of South American Earth Sciences* 2 (3), 207–222.
- Kent, D.V., Van der Voo, R., 1990. Palaeozoic palaeogeography from palaeomagnetism of the Atlantic-bordering continents. In: McKerrow, W.S., Scotese, C.R. (Eds.), *Palaeozoic Palaeogeography and Biogeography*. Geological Society Memoir, vol. 12, pp. 49–56.
- Kirschvink, J.L., 1980. The least squares line and plane and the analysis of paleomagnetic data. *Geophysical Journal of the Royal Astronomical Society* 62, 699–718.
- Kraemer, P., Escayola, M.P., Martino, R.D., 1995. Hipótesis sobre la evolución tectónica neoproterozoica de las Sierras Pampeanas de Córdoba (30°40′–32°40′) Argentina. *Revista de la Asociación Geológica Argentina* 50, 47–59.
- Lawver, L.A., Scotese, C.R., 1987. A revised reconstruction of Gondwana. In: McKenzie, G.D. (Ed.), *Gondwana Six: Structure, Tectonics, and Geophysics*. American Geophysical Union, Monographs, vol. 40, pp. 17–23.
- Lencinas, A., Timonieri, A., 1968. Algunas características estructurales del valle de Punilla, Córdoba. 3° Jornadas Geológicas Argentinas, Actas, vol. 1, pp. 195–207.
- Li, Z.X., Chen, Z., Powell, C., 1993. New Late Palaeozoic palaeomagnetic results from cratonic Australia, and revision of the Gondwanan apparent polar wander path. *Exploration Geophysics* 24, 263–268.

- Lira, R., Ripley, E.M., Españañ, A.I., 1996. Meteoric water induced selvage-style greisen alteration in the Achala Batholith, central Argentina. *Chemical Geology* 133, 261–277.
- McElhinny, M.W., Powell, Ch.McA., Pisarevsky, S.A., 2003. Paleozoic terranes of eastern Australia and the drift history of Gondwana. *Tectonophysics* 362, 41–65.
- McEnroe, S.A., Robinson, P., Panish, P.T., 2001. Aeromagnetic anomalies, magnetic petrology, and rock magnetism of hemo-ilmenite- and magnetite-rich cumulate rocks from the Sokndal Region, South Rogaland, Norway. *American Mineralogist* 86, 1447–1468.
- McFadden, P.L., McElhinny, M.W., 1990. Classification of the reversal test in palaeomagnetism. *Geophysical Journal International* 103, 725–729.
- McFadden, P.L., McElhinny, M.W., 1995. Combining groups of paleomagnetic directions or poles. *Geophysical Research Letters* 22 (16), 2191–2194.
- Meert, J.G., 2001. Growing Gondwana and rethinking Rodinia: a paleomagnetic perspective. *Gondwana Research* 4 (3), 279–288.
- Meert, J.G., 2003. A synopsis of events related to the assembly of eastern Gondwana. *Tectonophysics* 363, 1–40.
- Meert, J.G., Tamrat, E., 2004. A mechanism for explaining rapid continental motion in the Late Neoproterozoic. In: Eriksson, P.G., Altermann, W., Nelson, D.R., Mueller, W.U., Catuneanu, O. (Eds.), *The Precambrian Earth: Tempos and Events*. Elsevier Publications, pp. 255–266.
- Meert, J.G., Van der Voo, R., Powell, Ch.McA., Li, Z.X., McElhinny, M.W., Chen, Z., Symons, D.T.A., 1993. A plate-tectonic speed limit? *Nature* 363, 216–217.
- Morel, P., Irving, E., 1978. Tentative paleocontinental maps for the early Phanerozoic and Proterozoic. *Journal of Geology* 86, 535–561.
- Mutti, D., Di Marco, A., Geuna, S., 2007. Depósitos polimetálicos en el orógeno famatiniano de las Sierras Pampeanas de San Luis y Córdoba: fluidos, fuentes y modelo de emplazamiento. *Revista de la Asociación Geológica Argentina* 62 (1) pp.
- Otamendi, J.E., Castellarini, P.A., Fagiano, M.R., Demichelis, A.H., Tibaldi, A.M., 2004. Cambrian to Devonian geologic evolution of the Sierra de Comechingones, Eastern Sierras Pampeanas, Argentina: evidence for the development and exhumation of continental crust on the Proto-Pacific margin of Gondwana. *Gondwana Research* 7 (4), 1143–1155.
- Pinotti, L.P., Coniglio, J.E., Esparza, A.M., D’Eramo, F.J., Llambías, E.J., 2002. Nearly circular plutons emplaced by stoping at shallow crustal levels, Cerro Aspero batholith, Sierras Pampeanas de Córdoba, Argentina. *Journal of South American Earth Sciences* 15, 251–265.
- Piper, J.D.A., 2007. Palaeomagnetism of the Loch Doon Granite Complex, Southern Uplands of Scotland: the Late Caledonian palaeomagnetic record and an Early Devonian episode of true polar wander. *Tectonophysics* 432, 133–157.
- Ramos, V.A., 2004. Cuyania, an exotic block to Gondwana: review of a historical success and the present problems. *Gondwana Research* 7 (4), 1009–1026.
- Rapalini, A.E., 2005. The accretionary history of southern South America from the latest Proterozoic to the Late Palaeozoic: some palaeomagnetic constraints. In: Vaughan, A.P.M., Leat, P.T., Pankhurst, R.J. (Eds.), *Terrane Processes at the Margins of Gondwana*. Geological Society, London, Special Publications, vol. 246, pp. 305–328.
- Rapela, C.W., Heaman, L.M., McNutt, R., 1982. Rb–Sr geochronology of granitoid rocks from the Pampean ranges, Argentina. *Journal of Geology* 90, 574–582.
- Rapela, C.W., Toselli, A., Heaman, L., Saavedra, J., 1990. Granite plutonism of the Sierras Pampeanas; an inner cordilleran Paleozoic arc in the Southern Andes. In: Kay, S.M., Rapela, C.W. (Eds.), *Plutonism from Antarctica to Alaska*. Geological Society of America, Special Paper, vol. 241, pp. 77–90.
- Rapela, C.W., Pankhurst, R.J., Kirschbaum, A., Baldo, E.G.A., 1991. Facies intrusivas de edad carbónica en el Batolito de Achala: evidencia de una anatexis regional en las Sierras Pampeanas? 6º Congreso Geológico Chileno, Actas, pp. 40–45.
- Rapela, C.W., Pankhurst, R.J., Casquet, C., Baldo, E., Saavedra, J., Galindo, C., 1998a. Early evolution of the Proto-Andean margin of South America. *Geology* 26 (8), 707–710.
- Rapela, C.W., Pankhurst, R.J., Casquet, C., Baldo, E., Saavedra, J., Galindo, C., 1998b. The Pampean Orogeny of the southern Proto-Andes: Cambrian continental collision in the Sierras de Córdoba. In: Pankhurst, R.J., Rapela, C.W. (Eds.), *Proto-Andean Margin of Gondwana*. Geological Society of America, Special Publications, vol. 142, pp. 181–217.
- Robinson, P., Harrison, R.J., McEnroe, S.A., Hargraves, R.B., 2004. Nature and origin of lamellar magnetism in the hematite–ilmenite series. *American Mineralogist* 89, 725–747.
- Sato, A.M., González, P.D., Llambías, E.J., 2003. Evolución del orógeno Famatiniano en la Sierra de San Luis: magmatismo de arco, deformación y metamorfismo de bajo a alto grado. *Revista de la Asociación Geológica Argentina* 58 (4), 487–504.
- Schmidt, P., Powell, C., Li, Z.X., Thrupp, G., 1990. Reliability of Palaeozoic palaeomagnetic poles and APWP of Gondwanaland. *Tectonophysics* 184, 87–100.
- Siegesmund, S., Steenken, A., López de Luchi, M.G., Wemmer, K., Hoffmann, A., Mosch, S., 2003. The Las Chacras–Potrerillos batholith (Pampean Ranges, Argentina): structural evidences, emplacement and timing of the intrusion. *International Journal of Earth Sciences* 93 (1), 23–43.
- Simpson, C., Whitmeyer, S., De Paor, D., Gromet, P., Miró, R., Krol, M., Short, H., 2001. Sequential ductile to brittle reactivation of major fault zones along the accretionary margin of Gondwana in Central Argentina. In: Holdsworth, R., Strachan, R., Magloughlin, J., Knipe, R. (Eds.), *The Nature and Tectonic Significance of Fault Zone Weakening*. Geological Society, London, Special Publications, vol. 186, pp. 233–255.
- Sims, J.P., Ireland, T.R., Camacho, A., Lyons, P., Pieters, P.E., Skirrow, R.G., Stuart-Smith, P.G., Miró, R., 1998. U–Pb, Th–Pb and Ar–Ar geochronology from the southern Sierras Pampeanas, Argentina: implications for the Palaeozoic tectonic evolution of the western Gondwana margin. In: Pankhurst, R.J., Rapela, C.W. (Eds.), *The Proto-Andean Margin of Gondwana*. Geological Society, London, Special Publications, vol. 142, pp. 259–281.
- Steenken, A., Wemmer, K., López de Luchi, M.G., Siegesmund, S., Pawlig, S., 2004. Crustal provenance and cooling of the basement complexes of the Sierra de San Luis: an insight into the tectonic history of the Proto-Andean margin of Gondwana. *Gondwana Research* 7 (4), 1171–1195.
- Stuart-Smith, P.G., Camacho, A., Sims, J.P., Skirrow, R.G., Lyons, P., Pieters, P.E., Black, L.P., Miró, R., 1999. Uranium–lead dating of felsic magmatic cycles in the southern Sierras Pampeanas, Argentina: implications for the tectonic development of the proto-Andean Gondwana margin. In: Ramos, V.A., Keppie, J.D. (Eds.), *Laurentia–Gondwana Connections before Pangea*. Geological Society of America, Special Paper, vol. 336, pp. 87–114.
- Thrupp, G.A., Kent, D.V., Schmidt, P.W., Powell, C.McA., 1991. Palaeomagnetism of red beds of the Late Devonian Worange Point Formation, SE Australia. *Geophysical Journal International* 104, 179–201.
- Van der Voo, R., 1993. *Paleomagnetism of the Atlantic, Tethys and Iapetus Oceans*. Cambridge University Press, Cambridge. 411 pp.
- Van der Voo, R., 1994. True polar wander during the middle Paleozoic? *Earth and Planetary Science Letters* 122, 239–243.
- Vérard, Ch., Tait, J., Glen, R., 2005. Paleomagnetic study of Siluro-Devonian volcanic rocks from the central Lachlan Orogen: implications for the apparent pole wander path of Gondwana. *Journal of Geophysical Research* 110 (B06201). doi:10.1029/2004JB003287.